Crystal Structure and Charge Localization in $Pb_2Sr_2Ho_{0.625}Ca_{0.375}Cu_3O_8$

J.-E. Jørgensen[a] and N. H. Andersen[b]

[a] Department of Chemistry, Aarhus University, DK-8000 Århus C and [b] Risø National Laboratory, P.O. Box 49, DK-4000 Roskilde, Denmark

$Pb_2Sr_2Ho_{0.625}Ca_{0.375}Cu_3O_8$, which is isostructural with $Pb_2Sr_2HoCu_3O_8$, has been studied by neutron powder diffraction. The investigated sample was non-super-conducting. The Ca doping causes small structural changes. The overall symmetry is pseudo-tetragonal but stays orthorhombic. The structure of the PbO layers is almost unchanged, but the Pb–O bond is shortened. The out-of-plane Cu–O bonds are elongated, whereas the in-plane Cu–O bonds are slightly shortened. Calculations of bond valencies show that the valency of Cu in the CuO_2 layers is unaffected by the Ca doping but the Pb valency is increased. In addition, this family of compounds contains an oxygen-depleted Cu layer. The copper atoms in this layer are collinearly bonded to oxygen atoms in the PbO layers.

The family of $Pb_2Sr_2LnCu_3O_8$ compounds, where Ln represents a lanthanide ion, were discovered by Cava et al.,[1] and compounds have been prepared for all the naturally occurring lanthanides. Doping by a divalent ion, e.g. Ca^{2+}, results in hole-type high-temperature superconductors with critical temperatures close to 70 K. This family of compounds contain the structural elements that are characteristic for high-temperature superconducting copper oxides. The lanthanide ions are located between layers of corner-sharing CuO_5 pyramids. A similar structural arrangement is found in $YBa_2Cu_3O_7$ and in several bismuth- and thallium-based superconducting copper oxides. The stacking sequence in the $Pb_2Sr_2LnCu_3O_8$ family is $Ln–CuO_2–SrO–PbO–Cu–PbO–SrO–CuO_2–$. During low-temperature oxidation, oxygen is known to be incorporated in the Cu layer.[3] It is generally believed that the CuO_2 layers are of importance for superconductivity in high-T_c materials, and these layers are more separated in these materials than in, e.g., $YBa_2Cu_3O_7$. It is therefore to be expected that these compounds will show even more anisotropic properties than other high-T_c materials.

Previous X-ray and powder neutron diffraction studies of $PbSr_2YCu_3O_8$ and $Pb_2Sr_2HoCuO_8$ have shown that both compounds are pseudo-tetragonal but orthorhombic and contain distorted PbO layers.[4,5] The origin of the deviation from a tetragonal structure is the distortion of the PbO layers, which is due to the lone pairs located on the Pb^{2+} ions. These lone pairs are pointing towards the Cu layer. The aim of the present neutron powder diffraction study was to study the structural changes and charge localization caused by Ca doping. Special emphasis was given to the axial oxygen atoms which are located in the SrO layers and bonded to the Cu atoms in the CuO_2 layers, as well as to the Pb atoms in the PbO layers. These copper and oxygen atoms are labelled Cu(2) and O(1) in the following. The superconductivity of high-T_c cuprates is believed to be influenced of the axial oxygen atoms. It is reasonable to assume that the Cu(2)–O(1) distance is a sensitive probe of the amount of charge transfer from the PbO layers to the CuO_2 planes. Extensive powder neutron diffraction studies have shown that the corresponding distance in $YBa_2Cu_3O_{7-\delta}$ [usually labelled Cu(2)–O(4)] is correlated to the oxygen content.[6,7] Charge is transferred from the one-dimensional Cu–O chains to the CuO_2 layers in $YBa_2Cu_3O_{7-\delta}$ and the Cu(2)–O(4) distance decreases as δ approaches zero. An EXAFS study of $YBa_2Cu_3O_{7-\delta}$ has shown that the Cu(2)–O(4) interatomic potential in $YBa_2Cu_3O_{7-\delta}$ is highly anharmonic, suggesting that phonons as well as charge transfer are responsible for high-temperature superconductivity in this compound. This study showed that the Cu–O potential is of the double-well type and that a softening appears in the vicinity of the superconducting transition temperature.[8]

Experimental

The sample was prepared by firing a precursor of composition $Sr_2Ho_{0.625}Ca_{0.375}Cu_3O_{6.5}$ for 16 h at 980 °C in air. The precursor was mixed with PbO in the stochiometric ratio and pressed into pellets. The pellets were reacted in air for 1 h at 885 °C and rapidly cooled to room temperature. The sample was metallic, but turned out to be non-superconducting, although the corresponding Y-containing sample had been shown to be superconducting.[1] The lattice constants were determined from an X-ray Guinier film with Si as internal standard. All lines could be indexed on a C-centred orthorhombic cell with $a = 5.3851(9)$, $b = 5.4186(8)$ and $c = 15.752(3)$ Å.[9] The powder neutron diffraction
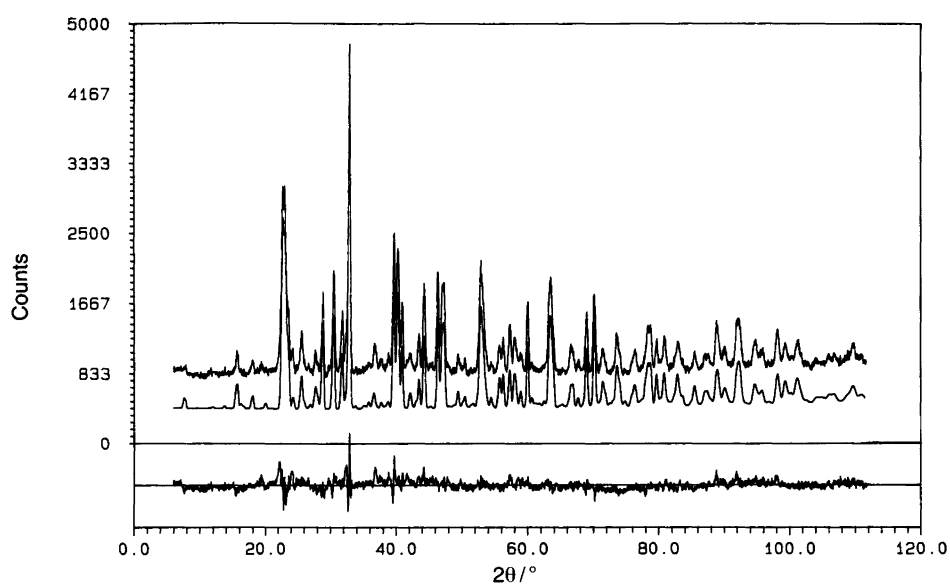
Fig. 1. Measured and calculated neutron diffraction profiles. The difference between observed and measured intensities is shown below. Data were recorded at room temperature.

experiment was performed on the multidetector powder diffractometer at Risø National Laboratory. Data were collected at room temperature, and the 711 reflexion from the Ge monochromator crystal was used for producing a monochromatic neutron beam of wavelength 1.079 Å. The directions of the incident and scattered beams are defined by Soller collimators of angular divergence 10 minutes of arc. The following neutron scattering lengths were used in the calculations b(Pb) = 9.401, b(Sr) = 7.02, b(Ho) = 8.08, b(Ca) = 4.7, b(Cu) = 7.718, b(O) = 5.805 fm. The Rietveld analysis was performed by aid of the program of Wiles and Young (version DBW 3.2S).[10]

located on the Ho site.[5] All atoms except the oxygen atoms O(2) and O(2′), located in the PbO layers, were constrained to obey C-centring. The occupation number for Ca in an Ho site did not refine to a meaningful value because of neutron absorption in Ho, and the chemical composition of the sample was assumed to be equal to the composition of the starting mixture. the observed and calculated diffraction profiles are shown in Fig. 1. The structural parameters are given in Table 1 and interatomic distances are given in Table 2; for comparison, the corresponding interatomic

Results and discussion

The crystal structure was refined in space group $P\bar{1}$ using the same model that was used for undoped $Pb_2Sr_2HoCu_3O_8$, and all Ca atoms were assumed to be

Table 1. Structural parameters $Pb_2Sr_2Ho_{0.625}Ca_{0.375}Cu_3O_8$.[a]

Atom	x	y	z	$B/Å^2$	Symmetry	
Pb	0.5	0.0	0.3866(3)	0.98(7)	4*l*	*mm*
Sr	0.0	0.0	0.2216(4)	0.67(7)	4*k*	*mm*
Ho/Ca	0.0	0.0	0.0	0.67(7)	2*a*	*mmm*
Cu(1)	0.0	0.0	0.5	1.1(1)	2*d*	*mmm*
Cu(2)	0.5	0.0	0.1067(4)	0.8(1)	4*l*	*mm*
O(1)	0.5	0.0	0.2559(5)	1.2(1)	4*l*	*mm*
O(3)	0.25	0.25	0.0952(3)	0.81(8)	8*m*	2
O(2)	0.06(1)	0.07(1)	0.388(3)	1.5(3)	2*i*	1
O(2′)	0.55(1)	0.45(1)	0.378(3)	1.5(3)	2*i*	1

[a]R_w = 8.59 %; R_{exp} = 4.02 %. Atomic positions above the dashed line have space group *Cmmm* symmetry, those below the dashed line have space group $P\bar{1}$ symmetry.

Table 2. Interatomic distances in $Pb_2Sr_2Ho_{1-x}Ca_xCu_3O_8$ (in Å).[a]

Atoms	x = 0.375	x = 0.0	No.
PB–O(1)	2.059(9)	2.129(9)	×1
Pb–O(2)	2.40(7)	2.39(4)	×1
Pb–O(2′)	2.46(6)	2.41(3)	×1
Pb–O(2)	3.04(6)	3.11(3)	×1
Pb–O(2′)	3.00(6)	3.03(3)	×1
Pb′–O(1)	2.059(9)	2.129(9)	×1
Pb′–O(2)	2.34(7)	2.19(4)	×1
Pb′–O(2′)	2.99(6)	2.92(3)	×1
Pb′–O(2)	3.12(6)	3.29(4)	×1
Pb′–O(2′)	2.43(6)	2.50(4)	×1
Sr–O(1)	2.746(2)	2.726(2)	×2
Sr–O(1)	2.763(2)	2.748(2)	×2
Sr–O(2)	2.67(4)	2.63(3)	×1
Sr′–O(2′)	2.50(4)	2.46(3)	×1
Sr–O(3)	2.759(5)	2.810(5)	×4
Ho–O(3)	2.428(3)	2.393(3)	×8
Cu(1)–O(2)	1.84(5)	1.91(4)	×2
Cu(1′)–O(2′)	1.96(5)	1.95(3)	×2
Cu(2)–O(1)	2.350(9)	2.272(9)	×1
Cu(2)–O(3)	1.918(1)	1.924(1)	×4

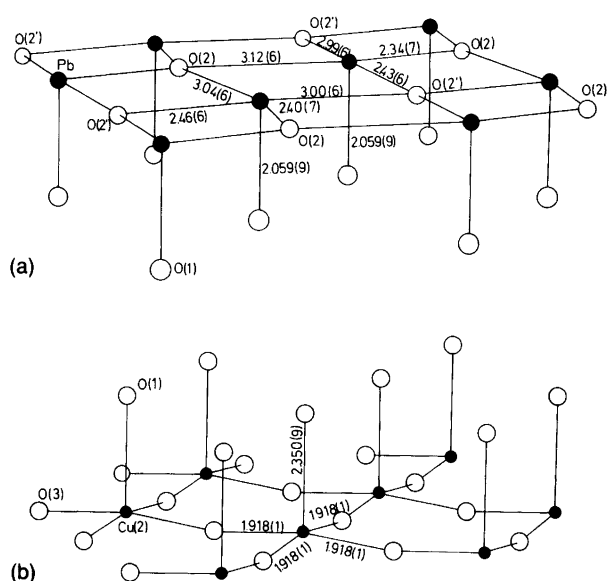[a]Cations marked with ′ are displaced by (1/2, 1/2, 0) from the positions given in Table 1.

Fig. 2. Connectivity and relevant interatomic distances (in Å) in the PbO layer (a) and the CuO$_2$ layer (b) in Pb$_2$Sr$_2$Ho$_{0.625}$Ca$_{0.375}$Cu$_3$O$_8$. The cations are marked with full circles and the oxygen atoms are marked with open circles. The oxygen atoms below and above the lead and copper atoms in (a) and (b), respectively, are the O(1) oxygen atoms. Oxygen atoms labelled O(2), O(2') and O(3) are located in the PbO and CuO$_2$ layers, respectively. Pb is five-coordinated with three short and two long Pb–O bonds. Cu is also five-coordinated with four short Cu–O bonds of equal length in the basal plane and one longer Cu–O bond perpendicular to the basal plane.

distances for undoped Pb$_2$Sr$_2$HoCu$_3$O$_8$ are included. The connectivity of the PbO and CuO$_2$ layers is shown in Fig. 2. Table 3 contains bond valencies for the cations in doped and undoped Pb$_2$Sr$_2$HoCu$_3$O$_8$ calculated according to Brown and Altermatt.[11]

The structural changes caused by Ca doping are minor. The lattice constant measurements show that the c-axis is elongated, whereas the orthorhombicity is unchanged within experimental error. The refinement of the powder neutron data shows that the distortion of the PbO layers is almost the same in doped and undoped Pb$_2$Sr$_2$HoCu$_3$O$_8$. The most remarkable structural change occurs in the CuO$_5$

Table 3. Bond valencies of cations Pb$_2$Sr$_2$Ho$_{1-x}$Ca$_x$Cu$_3$O$_8$.[a]

Atom	$x = 0.375$	$x = 0.0$
Pb	2.23	2.15
Sr	1.71	1.69
Ho/Ca	2.69	2.96
Cu(1)	1.12	1.02
Cu(2)	2.26	2.26

[a]Calculation of bond valencies for Ho/Ca and Cu(1) was done with $r_0 = 2.025$ and $r_0 = 1.679$, which are the empirical constants for Ho^{3+}–O^{2-} and Cu^{2+}–O^{2-} bonds, respectively.[11]

pyramids. The axial Cu(2)–O(1) distance is elongated by 0.078 Å in doped Pb$_2$Sr$_2$LnCu$_3$O$_8$ and the corresponding Pb–O(1) distance is shortened by 0.070 Å. The Cu(2)–O(3) distances are shortened by 0.006 Å. From Table 3 it is seen that the bond valency of Cu(2) is unchanged at the present level of Ca doping. The bond valency of Pb is on average increased from 2.15 to 2.23. This means that the present level of Ca doping causes a partial oxidation of the PbO layers, whereas the oxidation state of the CuO$_2$ layers is unchanged. It should also be remarked that the bond valency of the mixed Ho/Ca site is 2.69, whereas the bond valency of Ho in the undoped compound is 2.96. A bond valency of 2.63 would be expected from averaging the formal valencies of +3 and +2 of Ho and Ca, respectively, according to the stochiometric composition. The bond valency of Cu(1) is also enhanced from 1.02 to 1.12 by Ca doping, but it should be remarked that these values are somewhat uncertain because of the relatively large uncertainty of the O(2) and O(2') positions. A bond valency of 2.0 would be expected for Sr, but the relatively low values in Table 3 are presumably due to a structural mismatch between the SrO and PbO layers.

Studies of YBa$_2$Cu$_3$O$_{7-\delta}$ as a function of oxygen content have shown that the bond valency of Cu in the CuO$_2$ layers increases with increasing oxygen content and therefore is correlated with the variation of T_c with oxygen content. The axial Cu–O bond in the CuO$_5$ pyramids in YBa$_2$Cu$_3$O$_{7-\delta}$ decreases as δ approaches zero. This is in contrast to the behaviour found in Pb$_2$Sr$_2$Ho$_{0.625}$Ca$_{0.375}$Cu$_3$O$_8$, where the corresponding Cu(2)–O(1) distance is shortened at the present level of Ca doping. Both YBa$_2$Cu$_3$O$_{7-\delta}$ and Pb$_2$Sr$_2$HoCu$_3$O$_8$ contain charge reservoirs, and both doping and oxidation of these compounds can be understood in terms of the local charge picture.[12] The central idea of the local charge picture is that the superconducting CuO$_2$ layers are sandwiched between other layers which act as spacers and charge reservoirs. The electronic state of the charge reservoir controls the formal valency of the copper atoms in the CuO$_2$ layers and in this way the superconducting properties of the material. The formal and true charges on the copper atoms are of course different because of hybridization of the Cu 3d orbitals with the 2p orbitals on the oxygen atoms. Although being a hypothetical pictue, the local charge picture provides a good basis for understanding the doping mechanism in different copper oxides. The charge reservoirs in YBa$_2$Cu$_3$O$_{7-\delta}$ are the one-dimensional CuO chains. Oxygen vacancies are introduced in these chains in compounds with $\delta > 0$, resulting in charge transfer from the CuO chains to the CuO$_2$ planes. Charge transfer to the planes results in a reduction of T_c as well as the bond valency of the Cu atoms in the CuO$_2$ plains. The process is rather complex, and a two-plateau structure for T_c as well as the bond valency of the Cu atoms in the plains exists for $0 < \delta < 0.4$.[7]

The situation is somewhat different in Pb$_2$Sr$_2$HoCu$_3$O$_8$. Both the CuO$_2$ and PbO layers can be oxidized because of

the possibility of oxidizing Cu^{2+} and Pb^{2+} to Cu^{3+} and Pb^{4+}, respectively. The partial substitution of divalent Ca for trivalent Ho takes place next to the CuO_2 planes. Local charge neutrality could be preserved by oxidation of Cu in the CuO_2 planes, leaving the oxidation state of Pb unchanged. The present neutron diffraction study shows, however, that the process is more complicated. The PbO layer has been oxidized, whereas the oxidation state of Cu in the CuO_2 layers is left unchanged at the present level of Ca doping. The PbO layers are in this way working as a charge buffer, and a higher level of Ca doping will be needed to make $Pb_2Sr_2HoCu_3O_8$ superconducting. This is in accordance with other chemical evidence for Cu^{3+} being a stronger oxidating agent than Pb^{4+}. The structural changes induced by Ca doping are a useful probe for studing the changes in the local charge distributions.

The influence of axial oxygen atoms on the supercurrents on the CuO_2 layers is not yet understood. It has been suggested that a partial negative charge on the axial oxygen atom can enhance the pairing of electrons on the CuO_2 layers.[13] Experiments probing both the dynamical and statical properties of these oxygen atoms in different superconducting copper oxides are therefore of great interest. Low-temperature studies of the lattice stability of members of the present family of high-T_c materials would also be of importance for understanding the superconducting pairing mechanism in these materials. A study of charge localization in $Pb_2Sr_2YCu_3O_8$ as a function of the level of Ca doping is in progress.

References

1. Cava, R. J., Batlogg, B., Krajewski, Rupp, L. W., Schneemeyer, L. F., Siegrist, T., van Dover, R. B., Marsh, P., Peck, W. F., Jr., Gallagher, P. K., Glarum, S. H., Marshall, J. H., Farrow, R. C., Waszczak, J. V., Hull, R. and Trevor, P. *Nature (London) 336* (1988) 211.
2. Schneemeyer, L. F., Cava, R. J., James, A. C. W. P., Marsh, P., Siegrist, T., Waszczak, J. V., Krajewski, J. J., Peck, W. P., Jr. and Opila, R. L. *Chem. Mater. 1* (1989) 548.
3. Marezio, M., Santoro, A., Capponi, J. J., Hewat, E. A., Cava, R. J. and Beech, F. *Physica C 169* (1990) 401.
4. Cava, R. J., Marezio, M., Krajewski, J. J., Peck, W. F., Jr., Santoro, A. and Beech, F. *Physica C 157* (1989) 272.
5. Jørgensen, J.-E. and Andersen, N. H. *Acta Chem. Scand. 45* (1991) 19.
6. Cava, R. J., Batlogg, B., Sunshine, S. A., Siegrist, T., Fleming, R. M., Rabe, K., Schneemeyer, L. F., Murphy, D. W., van Dover, R. B., Gallagher, P. K., Nakahara, S., Farrow, R. C., Krajewski, J. J., Zahurak, S. M., Waszczak, J. V., Marshall, J. H., Marsh, P., Rupp, L. W., Peck, W. F., Jr. and Rietman, E. A. *Physica C 153-155* (1988) 560.
7. Jorgensen, J. D., Veal, B. W., Paulikas, A. P., Nowicki, L. J., Crabtree, G. W., Claus, H. and Kwok, W. K. *Phys. Rev. B 41* (1990) 1863.
8. Conradson, S. D., Raistrick, I. D. and Bishop, A. R. *Science 248* (1990) 1394.
9. Jørgensen, J.-E. *Powder Diffraction. In press.*
10. Wiles, D. B. and Young, R. A. *J. Appl. Crystallogr. 14* (1981) 149.
11. Brown, I. D. and Altermatt, D. *Acta Crystallogr., Sect. B 41* (1985) 244.
12. Cava, R. J. *Science 247* (1990) 656.
13. Bishop, A. R., Martin, R. L., Müller, K. A. and Tesanovic, Z. *Z. Phys. B 76* (1989) 17.